Bull. Spec. Astrophys. Obs., 1999, 48, 17-24

Pre- and post-flare evolution of AR 8038 on May 9 – 14, 1997 with Metsähovi–RATAN–BAO spectral microwave observations

V. Bogod[a], A. Grebinskij[a], V. Garaimov[a], S. Urpo[b], Q.J. Fu[c], H. Zhang[c]

[a] Special Astrophysical Observatory of RAS, St.Petersburg branch, Pulkovo, Russia
[b] Radio Research Institute, University of Helsinki, Helsinki, Finland
[c] Beijing Astronomical Observatory, China

Received February 22, 1999; accepted June 14, 1999.

Abstract. Eruptive destabilization of the solar corona and coronal mass ejections are central problems of solar physics. Currently, the search for realistic scenarios (in optics, X-rays and microwaves) of such events is far from being conclusive. Here we describe some new results of pre-flare mass and energy build-up for the AR NOAA 8038 on May, 1997, based on broad-band (about 1–87 GHz) microwave cooperative studies with the facilities of RATAN–600 (spectral observations), Metsähovi (millimeter band imaging), and Beijing astronomical observatory (time profiles of the burst event at 2.84 GHz and vector magnetograph observations). This AR was a perfectly useful object for study of energy build-up scenarios because it produced only one major flare event (near 05 UT on May 12, 1997). Microwave study of pre- and post-flare ARs gives an opportunity of detection of evolution changes from chromosphere to coronal structures. The main finding of this report concerns the unusual behaviour of coronal emission evolution. For three days before the flare event its brightness was steadily decreasing and steadily growing for three days after the event to the same final level. Our results point to strong thermal instability of the AR before the flare and may be interpreted as an indication of significant steady flows from the photosphere to the corona with a significant mass build-up before the flare.

Key words: Sun: corona - Sun: evolution - methods: observational

1. Introduction

Many solar phenomena (flares, coronal mass ejections (CMEs), filament eruptions) involve large-scale destabilization of the corona. Statistical scenarios based on fragmented energy release on the microscales (see Vlahos, 1995 for review), enabled us to discover a physical origin of solar explosive activity. Diagnostics of energy build-up and prediction of such phenomena are also open to question.

Different scenarios of energy build-up (active regions with a well developed current system or moving magnetic footpoints via random photospheric fluid motions) presume short (hours) time scales (see Hanaoka, 1997). Such scenarios do not explain the significant mass concentration in the corona, well observed as its post-flare ejection, which needs steady mass inflows from the photosphere to the corona. The relation between various pre-flare energy build-up scenarios and types of primary flare energy release (impulsive, gradual and especially violent (Li and Fu, 1996)), microwave diagnostics of proton events and the flare origin is an important problem also.

Here we consider the evolution of the active region AR 8038 on May 9-14, 1997 at microwaves.

This AR is an especially interesting object for studying the nature and scenarios of flare activity. The AR produced only one major flare event (near 04:59 UT on May 12, 1997) during its passage across the solar disk, which gives a rare opportunity to study the different manifestations of pre-flare energy build-up and its post-flare relaxation. The flare had a significant energy release in the corona (II Type bursts, shocks and, possibly, CME events were reported).

The event under consideration was one of the first active regions in the new 23-d solar activity cycle and there is a good opportunity of using the last technical improvements for cooperative studies and new observational techniques. It was a particularly suitable object to observe with the RATAN-600, a fan-beam multi-wave instrument, owing to the extremely low activity of the source in other parts of the solar disk. Apart from the RATAN-600 data (30 frequencies at 0.9–14 GHz in intensity and polarization), we used the

information from the cooperative observations of this event with Metsähovy imaging (80 GHz, in intensity), Beijing Radio Station (2.84 GHz, in intensity), optical vector-magnetography (Huairou Station of BAO), together with regular X-ray (BATSE) and microwave (Nobeyama 17 GHz Radioheliograph) observations. Observational testing of different flare scenarios in optics are rather inconclusive because of the stability of photospheric magnetic field structures before and after the flare events. The hot coronal plasma is confined in magnetic loops, SXR and EUV loops. It provides useful tracers of the magnetic field and electric currents (see Aschwanden, 1995 for review). A quantitative comparison with potential field calculations (Sakurai et al., 1992) for a SXR loop observed before and after the flare demonstrates that the S-shaped (sheared) loop before the flare corresponds to a non-potential configuration, while the (relaxed) post-flare loop is stipulated by a dipole potential field. However, a comparison of SXR loops (Yohkoh images) with ground-based vector magnetograph data shows (Metcalf et al., 1994; Zhang, 1995) that the relation between the SXT structures and the distribution of vertical electric currents in the AR is not simple. Microwave study of post-flare AR emission gives an opportunity of detection of the structural changes from the deep chromosphere to the corona. In a shorter wavelength range (mm–cm) we have bremstrahlung radiation of the chromosphere, and at longer wavelengths (cm) we can study gyroresonance emission of AR magnetospheres from the transition region to the corona.

In this paper we give preliminary results of a phenomenological study of the AR 8038 evolution. The main finding of our report is a rather unexpected trend in evolution of microwave emission of the AR. For 3 days before the flare event, its brightness was steadily declining at all wavelengths (from chromosphere to corona levels), and vice versa, for 3 days after the flare event, emission was steadily growing. It is also important, that some specific spectral details in the emission spectrum (see, for example, Bogod et al., 1999), clearly manifested in the RATAN observations on May 9, were smoothed out to May 11, a day before the flare event time on May 12, and were fully restored at the same frequencies two days after the flare event in the May 13–14 observations.

We will preliminarily discuss such trends as indications of magnetic stability of the AR 8038. The trends are accompanied by change of the thermal conditions of AR due to possible upflows of cool matter from the photosphere to the corona before the flare and some downflows at the post-flare stage. Using the combined spectral RATAN-600 and time-resolved Metsähovi observations, we studied near post-flare (with lags of several hours) energy release at 07–09 UT on May 12. In the paper we are trying to identify

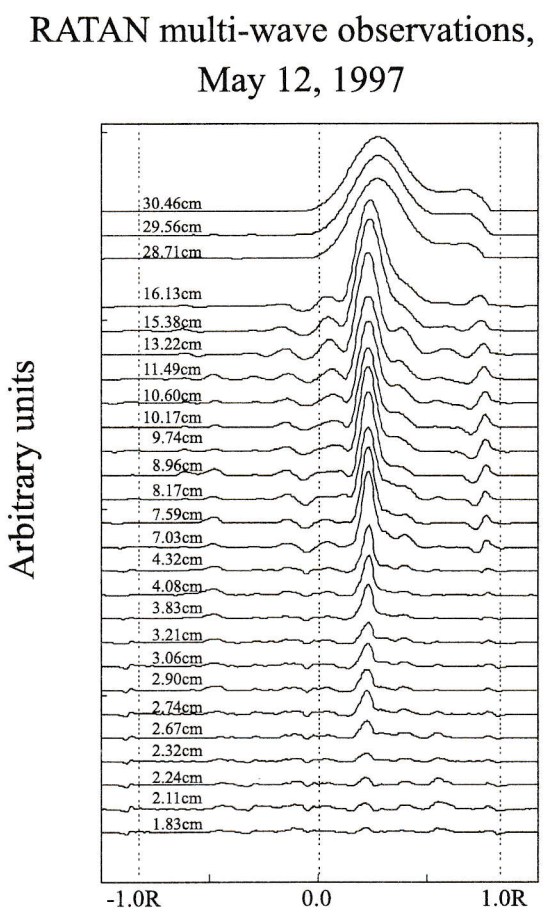

Figure 1: *Spectral presentation of S-component. Emission of the quiet Sun is subtracted.*

the primary energy release pattern during the flare event with its microwave (BAO observations at 10.7 cm) and hard X-ray (BATSE) burst emission on May 12 and to find its relation with the discussed pre-flare energy build-up scenario.

Finally, we will discuss our findings in relation with photospheric optical observations on the Huairou vector magnetograph of BAO (see Zhang, 1994), to find indications of upflows and downflows for the observed AR evolution pattern.

2. Observations and data reduction

The active region AR 8038 was located near CM (N21 W09) on May 12, 1997 and had a very high flare activity. A major flare was recorded in H_α at 0445–0632 UT, with the peak activity around 0452 UT, which was classified as 1N in optics and C 1.3 in X-rays. The flares were accompanied by radioevents of I, II, III and IV spectral classes in the same time interval according to the SGD bulletin. In the meter waveband, the activity of I and III spectral type lasted until 17 UT with the peak at about 12 UT.

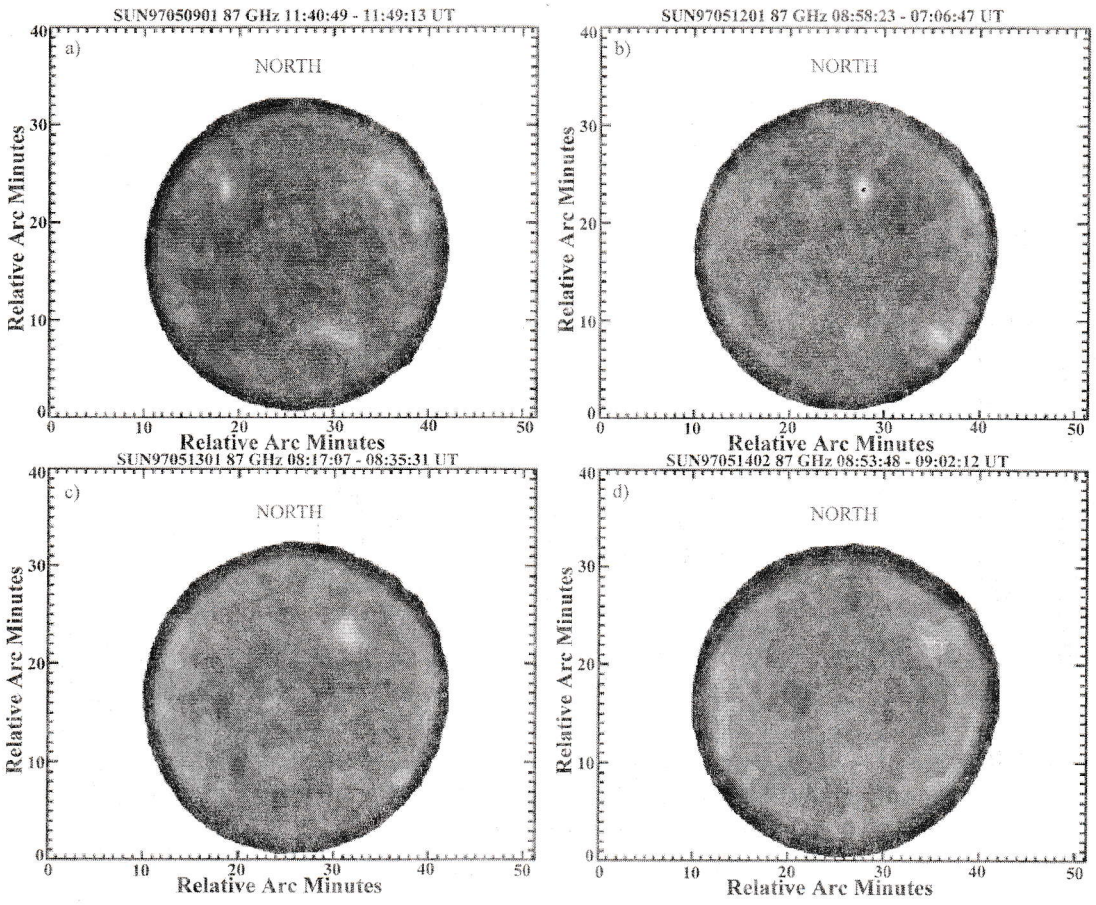

Figure 2: *Metsähovi solar maps: a) May 9, b) May 12, c) May 13 and d) May 14.*

On May 13 only weak activity was recorded by GOES observations. On May 9–11 no activity was reported.

We observed AR 8038 with a fan-beam diagram of the RATAN-600 in the wavelengthband $\lambda = 1.83 - 30.46$ cm at 09 UT daily from May 9 to 14 (see example in Fig. 1). These observations were accompanied by Metsähovi Radio Research Station cooperative observations on May 9, 12–14. Here, the 14-meter single-dish antenna was used in the sub-mm band at $\lambda = 0.3$ cm (87 GHz) with a series of full-Sun disk maps. On May 12, 6 maps were obtained at 6:58–12:37 UT, and on May 13, 5 at 8:17–12:18 UT. Examples of Metsähovi images are shown in Fig. 2. The time interval of our microwave observations on May 12, 1997 refers to the post-flare activity of the AR 8038.

Time profiles of the flare event were recorded in Nobeyama and Beijing at microwaves and with the Cosmic missions. 2.84 GHz patrol observations in BAO on May 12 were started at 04:47:14 UT (see time profile in Fig. 3a), just several minutes before the onset of the microwave event and the accompanying optical flare. As a primary energy release indicator, we used the hard X-ray time profile from the BATSE experiment, channel 25.0–50 keV. This profile (see Fig. 3b) suggests a gradual type energy release pattern between 04:48–04:58 UT with strong temporal fragmentation.

2.1. Data reduction with Metsähovi observations

Full-disk images on May 9, 12 and 13 are presented in Fig. 2a–d. All images were constructed using separate scans by moving the dish with a main beamwidth of about 60″ at f = 87 GHz during a 12 minutes' cycle. Full images were processed to construct brightness contour maps relative to the estimated brightness of the quiet Sun. Our resolution is sufficient for study of large-scale structures (such as plage areas). We do not apply any reduction of images for diagram smoothing, so we would analyze here only the observed excesses of the antenna brightness temperature.

In the location of the AR 3038 on the maps presented we see excesses of about 0.04–0.06 relative to the quiet Sun brightness in a single elongated brightness source. We see also the clear brightness enhancement both for the nonflaring days on May 9, 13 and on May 12 images. We processed these peak bright-

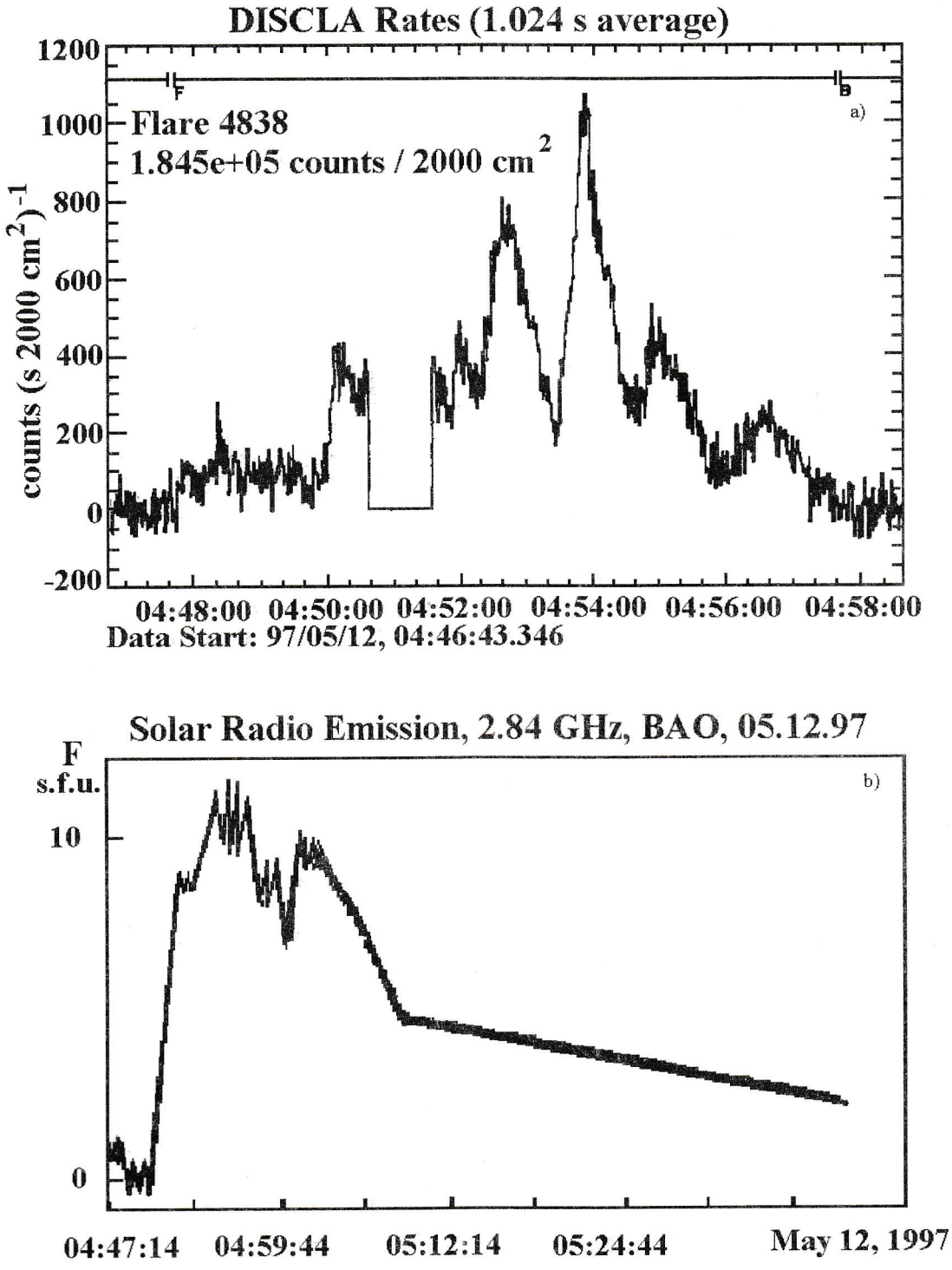

Figure 3: *a) – activity of AR8038 in X-rays according to BATSE (25–50 keV); b) – time profiles for the flare event on May 12, 1997, at 2.84 GHz.*

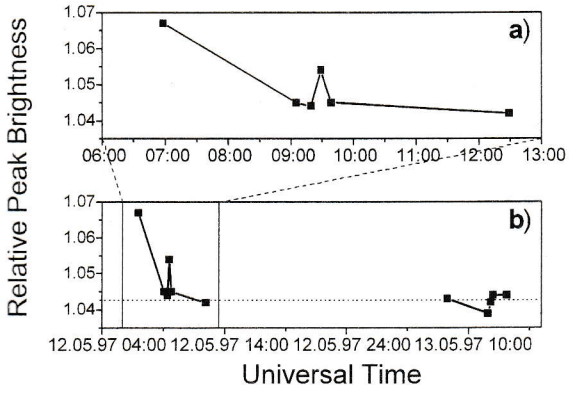

Figure 4: *History of AR8038 according Metsähovi data: a) May 9, 1997; b) May 12–13, 1997.*

Table 1: *Metsähovi observations.*

Day	Time UT	Peak
12/5/97	6:58–7:06	1.067
	9:05–9:13	1.045
	9:19–9:28	1.044
	9:29–9:37	1.054
	9:39–9:47	1.045
	12:29–12:37	1.042
13/5/97	8:17–8:25	1.043
	11:36–11:44	1.039
	11:50–11:58	1.042
	11:59–12:08	1.044
	12:09–12:18	1.044

ness excesses for all maps (see Table 1).

The temporal history of brightness excess evolution of the AR 8038 sub-mm emission is separated on two different time-scales: (a) as a short-term at 9:05–12:29 UT, May 12 (Fig. 4a), just after the X-ray event (around 04:54 UT, May 12), and (b) as a long-term from 04:50 UT, May 12 to 12:09 UT, May 13 (Fig. 4b).

The accuracy of the measurements of the observed brightness excesses is estimated to be within ±0.002.

2.2. Data reduction of RATAN-600 observations

The multiwave one-dimensional scans of antenna temperatures were calibrated to daily total fluxes of the Sun and then transformed to the scans for full intensity (see Fig. 1). After subtraction of the quiet Sun, it is possible to calculate the flux spectra and estimate the brightness spectra of local emission sources. Here we restrict our study to evaluations of peak brightness of the source in terms of calibrated antenna temperatures. Because we are interested in small day-to-day brightness variations, such an approach gives the best accuracy.

For each day of observations in the frequency band

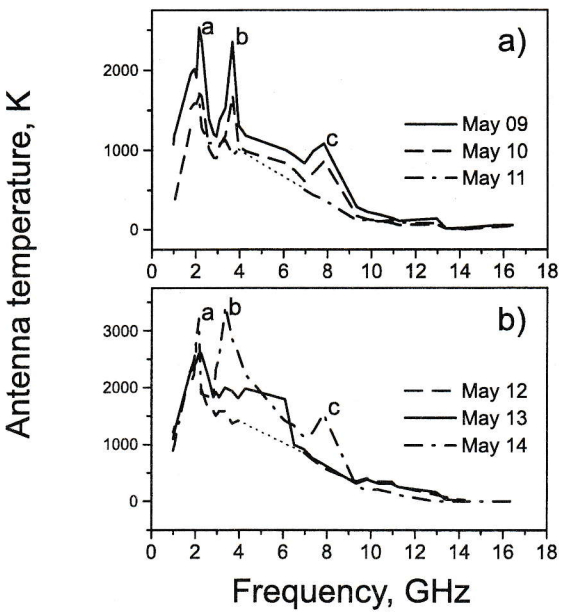

Figure 5: *Brightness spectra of AR8038 in the range 1.0 – 16 GHz according RATAN observations during May 9 – 14, 1997. Dotted line means the interpolation in the part of spectra without data.*

1.0–16 GHz, we constructed the brightness spectra which were grouped for three days (May 9–11) before the flare (see Fig. 5a) and three days (May 12–14) after it (see Fig. 5b). The data presented demonstrate the sharp brightness at frequencies below 10 GHz, which we consider as transition from weak chromosphere emission to strong coronal emission. Also, one can see several narrow band spectral enhancements on the spectra and some systematic brightness variations between consecutive spectra. The error bars do not exceed 10 %. For further discussions, we label the most prominent spectral peaks by (a), (b) and (c) in order to refine their wavelength locations. As it is seen from the observed profiles (see Fig. 5 a and b), the intensity peaks of the source are located at the same frequencies. The polarization emission demonstrates strong westward displacements, which grow with wavelength. But we would like to restrict our study here only to consideration of the intensity emission component.

2.3. Photospheric magnetograms

In Fig. 6 we show the results of photospheric observations with the vector magnetograph of the Beijing observatory (Huairou Solar station) for a few days. This data set includes two days before and one day after the flare on May 12 to illustrate stability of the magnetic structure of the AR under study. No rise in the magnetic flux was observed around the time of

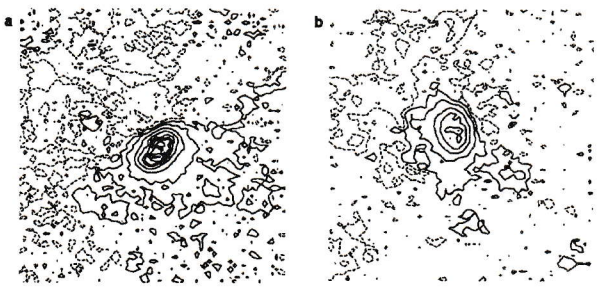

Figure 6: *Photospheric longitudinal magnetograms in the active region NOAA 8038 for May 9 (left) and May 13 (right) 1997. The solid (dashed) contours correspond to positive (negative) fields of 40, 160, 640, 1280, 1920, 2240 Gauss.*

the flare.

3. Results of observations

Observations of pre- and post-flare emission for the same AR in a wide frequency band, 87–1.5 GHz, give a possibility of studying the solar atmosphere evolution from deep chromosphere to corona. As a preliminary report, we present results of such studies separately for the chromosphere and corona evolution.

3.1. Chromosphere post-flare response

Sub-mm study of flare ARs is important for discovery of dominating sites of primary flare energy release (chromosphere or coronal events). From the X-ray observations with the Yohkoh facilities and microwave imaging with the Nobeyama radioheliograph at 17 GHz the simultaneous brightening at the top- and footpoints of flaring loops is known. But such observations alone, and only for the flare phase, are insufficient to answer all questions. Indeed, X-ray enhancements relate either to the hottest plasmas (thin target) or to the upper chromosphere bremstrahlung (thick target mechanism). Microwave emission from the foot-points of the loops also originates predominantly in the upper chromosphere (as bremstrahlung emission of evaporated plasma, or nonthermal synchrotron). On the other hand, the microwave brightening in the sub-mm band are related to the deep chromosphere, with electron temperatures of about 7000 K, versus 15000 K in the upper chromosphere. Such layers are dense and have a very short (minutes) cooling time (see Schmieder et al., 1995 for review), so any sub-mm brightness enhancements may suggest the energy release (pulsed or continuous) to be of chromosphere origin.

In the Metsähovi observations we found 2 clear enhancements (Fig. 4a) just after the main flare event, with a rather smooth background (Fig. 4b). The first enhancement, which is about 1.5 times stronger relative to the quiet AR contrast, was recorded only on one map at 6:58–7:06 UT. Due to the gap in the cycle of mapping, the next map was drawn about 2 hours later (and does not show any additional brightness contrast, see Table 1). So, for this case we are unable to evaluate the cooling time. Possible relation of this brightening with the main flare event (two hours before) is unknown either.

The case of the second brightening is much more conclusive. It occurred during the 3 consecutive mappings, which were taken within 28 minutes. The brightness enhancement (about 0.054 on the map between 9:29 and 9:37 UT) is relatively small, but clearly defined against the smooth background of the adjacent maps (with the same enhancement of about 0.044 ± 0.001, see Table 1).

We can suggest that if this event is related to impulsive input of energy in the deep chromosphere, its characteristic time scale for rise and cooling is less than 10 minutes. This information may be very useful for the energy transport problems and energy balance in the deep chromosphere. The total input energy for such events can be estimated on the basis of the current deep chromosphere models. The time of the second post-flare Metsähovi mapping (9:05–9:13 UT) on May 12 coincided with the RATAN-600 observation (around 9:10 UT). As it is seen from the RATAN-600 spectra (Fig. 5), the observations do not show any brightness enhancements at the shortest waves, near 12–16 GHz, because of the low temperature resolution of fan-beam observations of weak emission sources. So, a comparison of the Metsähovi and RATAN-600 observations leads to an important conclusion concerning the nature of emission enhancement for such sources in the deep chromosphere.

3.2. Coronal pre- and post-flare response

The emission spectra with the RATAN-600 observations presented in Fig. 5 reveal a rather peculiar pattern of the AR microwave evolution before and after the flare event, with two characteristic features.

1. As it is seen from the pre-flare spectra, the emission in all frequency bands was steadily decreasing before the flare, and vice versa, steadily growing after the flare. Thus, the flare condition in this AR is related to a minimum of microwave emission. Such brightness drops before flares had been detected earlier and considered as flare precursors. In this study we traced such effects using wide-frequency-range observations and, for the first time, traced them on long-time scales.

2. The second conclusion relates to the evolution of fine-structure spectral patterns of microwave emission. As one can see from Fig. 5, the flare spectra on

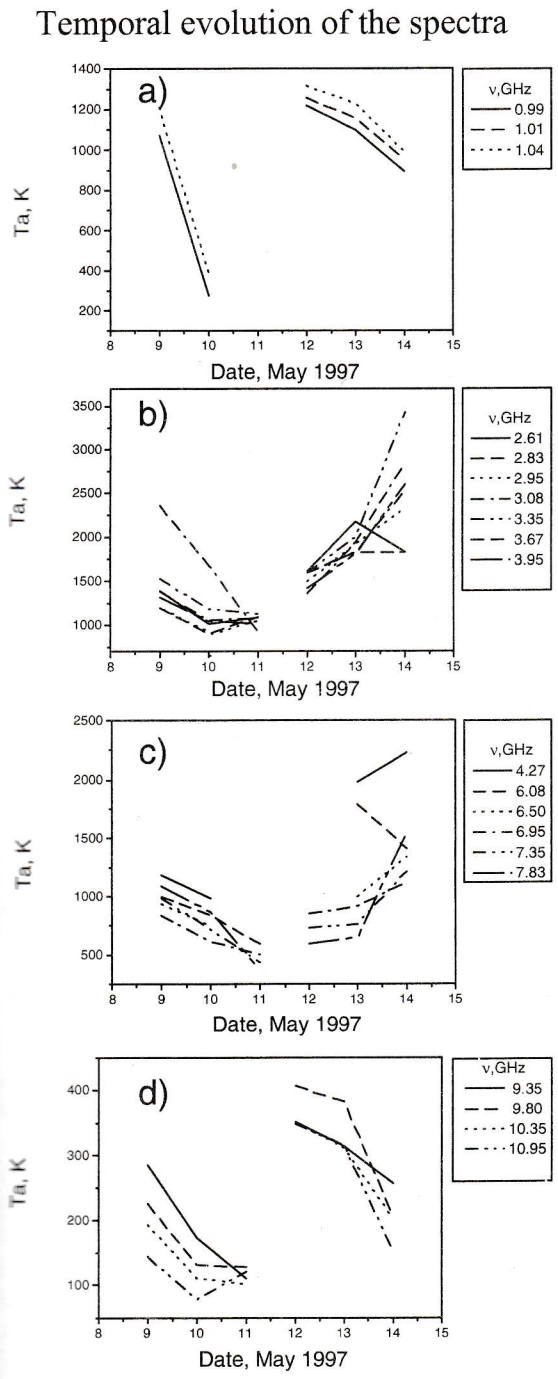

Figure 7: *The temporal evolution of different parts of the microwave wide range spectra during May 9–14, 1997. The part of the spectra associated to a) the coronal loop top emission; b) the sunspot coronal emission; c) the transition region emission; d) the sunspot chromosphere emission.*

May 9 (3 days before) and on May 14 (3 days after) have clear peaked spectral patterns with 3 peaks, A, B and C, at the same frequencies. But, at the time close to the flare (on May 11, a day before, and on May 12, a day after) all spectral peaks were smoothed out. Thus, according to the RATAN-600 spectra the flare is a state with a minimum microwave emission and without any spectral peculiarities.

As regards the time evolution, this may suggest that the observed microwave evolution is mainly due to the thermal evolution (total cooling) of the AR before the flare. At the same time, the magnetic structure stays practically unchanged before, near and after the flare. The restoration of all peculiar spectral details on the third day after the flare event points to this fact. The disappearance and reappearance of fine spectral details suggest a complex loop structure of the AR 3038. We detailed the picture of AR 3038 evolution in different frequency bands in Fig. 7. Fig. 7a presents the variation of brightness during May 9–14 at fixed frequencies (0.99–1.01 GHz), which may be related to the coronal loop emission. In Fig. 7b we show the same for the frequencies 2.15–3.95 GHz related to coronal plasma above the spot area, in Fig. 7c for transition region emission (4.27–7.83 GHz), and in Fig. 7d for the upper chromosphere emission (9.35–10.95 GHz). Such an interpretation of emission sources is based on their relative brightness patterns. From examination of data presented in Fig. 7 we see several evolution behaviours. The pre-flare brightness decreasing is observed at all levels and frequency structures of the AR, but the post-flare evolution is different.

- Just after the flare (4 hours later, May 12), the observed brightening is the most prominent in the coronal loops and in the chromosphere (Fig. 7a, d), but almost absent in the corona and transition region (TR) (Fig. 7b, c).

- The post-flare (May 13–14) evolution of the structures mentioned above is also quite different: we observe a steady cooling of the coronal loops and chromosphere (Fig. 7 a, d), but the brightening is steady in the corona and TR (Fig. 7 b, c).

Such flare brightening patterns for the coronal loops and chromosphere are not unusual, if the primary flare heating is localized at the top and feet of a coronal loop, as follows from many X-ray observations. However, the existence of the strong brightness drops at all levels of the AR before the flare is a new and unexpected pattern. Upflows of cool chromosphere matter with possible triggering of current disruption at the flare onset may be one of the reasons.

3.3. Pre-flare evolution and primary energy release pattern

The detected pre-flare evolution patterns may be interpreted as significant mass upflows, which is an important factor in the total energy build-up. This scenario differs much from the currently used scenarios with magnetically interacting loops, but it can explain the strong mass ejections at the flare stage and the strong magnetohydrodynamic turbulence in the course of energy release. As it was mentioned above (Li and Fu, 1996), such a pattern of primary energy release may lead to the events with strong mass and proton ejections in outer space. Using the time-profile patterns of primary energy release one can realize diagnostics of the flare stage. Our observations provide strong support for such a hypothesis: time profiles of the flare (see Fig. 3 a, b) display strong fluctuations of energy release both in hard X-rays and at microwaves.

4. Discussion and conclusions

Cooperative observations of solar microwave emission with Metsähovi–RATAN-600–BAO facilities give new information on many important problems of solar flare activity origin from the deep chromosphere to the corona, as has been discussed herein. A comparison of photospheric magnetograms and microwave spectra confirms the importance of a new scenario of flare energy build-up, which is based on steady states of magnetic fields and changes in the thermal conditions in the solar active region. This scenario is in favour of the current-disruption flare models (Zaitsev and Stepanov, 1991) with a stable configuration of the AR magnetic field structure, but with significant pre-flare mass inflows and violent mass ejection into outer space.

Acknowledgements. This programme of research has been partially supported by the Russian Foundation for Basic Research (RFBR) Projects 99-02-16403a and INTAS - RFBR grant 95-0316 and Federal Russian Programme "Astronomy".

References

Aschwanden M.J., 1995, Proc. CESRA Workshop on Coronal Magnetic Energy Releases, eds. A.O. Benz and A. Krueger, Lecture Notes in Physics, **444**, 13

Bogod V.M., Garaimov V.I., Zheleznyakov V.V., Zlotnik E.Ya., 1999, Proc. Of Nobeyama Symp. 1998, NRO Report

Hanaoka Y, 1997, Solar Physics, **173**, 319

Li Chun-sheng, Fu Qi-jun, 1996, Chin. Astron. Astrophys., **20**, No.1, 69

Metcalf T.R., Canfield R.C., Hudson H.S., Mickey D.L., Wuelser J.P., Martens P.C.H. and Tsuneta S., 1994, ApJ, **428**, 860

Sakurai T., Shibata K., Ichimoto K., Tsuneta S., Acton L.W., 1992, PASJ, **44**, L123

Schmieder B., Heinzel P., Wiik J.E., Lemen J., Anwar B., Kotrc P. and Hiel E., 1995, Solar Phys., **156**, 337

Vlahos L., 1995, Proc. CESRA Workshop on Coronal Magnetic Energy Releases, eds. A.O. Benz and A. Krueger, Lecture Notes in Physics, **444**, 115

Zhang Hongqi, 1994, Proc. of the Third Workshop on Solar Magnetic and Velocity Fields, 25

Zhang Hongqi, 1995, Astron. Astrophys, **304**, 541

Zaitsev V.V., Stepanov A.V., 1991, Astron. Zh., **68**, 384